

Low Resistance III-V Heterocontacts to N-Ge

Junkyo Suh¹, Pranav Ramesh¹, Andrew C. Meng², Aravindh Kumar¹, Archana Kumar¹, Shashank Gupta¹, Raisul Islam¹, Paul C. McIntyre², and Krishna Saraswat^{1,2}

¹Department of Electrical Engineering, Stanford University, Stanford, CA 94305, U.S.A.

²Department of Material Science & Engineering, Stanford University, Stanford, CA 94305, U.S.A.

E-mail: {suhjk, saraswat}@stanford.edu

Abstract: We experimentally study III-V/Ge heterostructure and demonstrate InGaAs heterocontacts to n-Ge with a wide range of In % and achieve low contact resistivity (ρ_c) of $5.0 \times 10^{-8} \Omega \text{cm}^2$ for Ge doping of $3 \times 10^{19} \text{cm}^{-3}$. This results from re-directing the charge neutrality level (CNL) near the conduction band and benefiting from low effective mass for high electron transmission. For the first time, we observe that the heterointerface presents no temperature dependence despite the two different conduction minimum valley locations of III-V (Γ -valley) and Ge (L -valley), which potentially stems from elastic trap-assisted tunneling through defect states at the interface generated by dislocations. The heterointerface plays a dominant role in the overall ρ_c below $\sim 1 \times 10^{-7} \Omega \text{cm}^2$, which can be further improved with large active dopant concentration in Ge by co-doping.

Introduction: Ge is a promising material for future CMOS because of its inherently superior carrier mobility and light effective mass. However, large parasitic contact resistance to n-Ge exists due to metal Fermi-level pinning near the valence band [1] and its low dopability (Fig. 1). Attempts to minimize this mainly fall into two categories; 1) interlayer placement between metal and Ge to reduce barrier height [2] and 2) increasing active dopant concentration (N_d) by co-doping [3] and/or laser annealing [4]. Laser annealing especially greatly improves dopant activation in Ge above $1 \times 10^{20} \text{cm}^{-3}$, but, the benefits vanish during subsequent thermal cycles due to poor thermal stability. On the other hand, the interlayer placement has recently shown great promise in lowering ρ_c to n-Ge by exploiting well-established Ti(Si_x)/Si:P on n-Ge [2].

In this study, we propose III-V as an interlayer and systematically investigate the heterocontact from material and electrical characteristics standpoints. III-V is favorable in that the CNL is located near the conduction band as well as its low effective mass, beneficial for high electron transmission. High In % space was explored (Fig. 2), resulting in nearly zero barrier height [5]. More importantly, we study the temperature dependence of the heterocontact to understand possible carrier transport mechanism at the heterointerface where carriers have to travel across different valleys (Γ to L and vice versa). It was found that the heterointerface presents no temperature dependence, which may be indicative of elastic trap-assisted tunneling through defect states from dislocations.

Experiment: Ge was epitaxially grown on (100) n-Si [6]. In order to evaluate ρ_c with high precision, MRCTLM structure was fabricated [7]. The key process steps are delineated in Fig. 3. There are two groups of n-Ge doping in terms of N_d ; 1) in-situ PH₃ with N_d of $5 \times 10^{18} \text{cm}^{-3}$ during Ge epitaxy and 2) ion implantation (I. I.) with N_d of $3 \times 10^{19} \text{cm}^{-3}$. Mo was chosen as contact metal [8] followed by W/Al metallization.

Results and Discussion

A. Material Characteristics of III-V Heterocontacts to n-Ge

3D island growth of InGaAs on Ge was observed with dislocations due to large lattice mismatch (Fig. 4). The surface

becomes rougher with In up to 80% and plateaus (Fig. 5). As a result of complete strain relaxation, large FWHM (Fig. 6) and mosaicity (Fig. 7) of III-V were observed by XRD. The estimated threading dislocation density is $\sim 1 \times 10^{10} \text{cm}^{-2}$ by Kuhn's model [9] (Fig. 8). HRTEM & EDS analyses were performed, which is consistent with XRD (Fig. 9).

B. Electrical Characteristics of III-V/n-Ge Contact

The heterocontact exhibits ohmic behavior and ρ_c was extrapolated from resistance vs. ring spacing plot (Fig. 10). It was found that ρ_c remains high at 60% In regardless of N_d in Ge due to high R_{contact} whereas the effects of the heterointerface ($R_{\text{heterointerface}}$) on ρ_c start to manifest above 70% In as a function of N_d in Ge (Fig. 11). It should be pointed out that ρ_c of the group with higher N_d in Ge (I.I.) keeps decreasing with higher In % as opposed to that with lower N_d (in-situ PH₃), which means that $R_{\text{heterointerface}}$ plays a dominant role in total ρ_c below $1 \times 10^{-7} \Omega \text{cm}^2$ and $R_{\text{heterointerface}}$ can be engineered by higher N_d in Ge. Low ρ_c of $5.0 \times 10^{-8} \Omega \text{cm}^2$ was achieved at InAs/n-Ge with N_d of $3 \times 10^{19} \text{cm}^{-3}$, which could be further enhanced with larger N_d by co-doping (Fig. 12). Moreover, optimization of III-V growth temperature is crucial for low ρ_c (Fig. 13).

Understanding of the heterointerface and carrier transport mechanism is critical to be able to engineer $R_{\text{heterointerface}}$, and thus the temperature dependence was examined. Since III-V and Ge have different minimum valleys (III-V/Ge systems without crystalline imperfections), carriers have to transit to the other valley across the interface by changing energy and momentum in E-k space, which adds high parasitic $R_{\text{heterointerface}}$ [2] because of intervalley scattering which is a function of temperature. However, the heterointerface presents no temperature dependence (Fig. 14), which is possibly attributed to carrier conduction through defect states generated by dislocations [10]. It is plausible that misfit dislocations and/or point defects near the heterointerface lead to energy states in the band-gap [10], which assists carrier transport between Γ and L with no need of temperature dependence. Our proposed band [11] and E-k diagrams are illustrated in Fig. 15. Our data may be concrete evidence that the momentum change may occur through defect states.

Conclusions: The III-V heterointerface with Ge and its heterocontacts to n-Ge were systematically investigated. Low ρ_c of $5.0 \times 10^{-8} \Omega \text{cm}^2$ was achieved, which could be further improved by co-doping (Fig. 16). The heterointerface was found to show no temperature dependence which is suggestive of elastic trap-assisted carrier transport at the interface through defect states.

Acknowledgement; This work was supported by Stanford INMP, Global Foundry, TSMC & Lam Research. **References;** [1] T. Nishimura et al., APL, 91 (2007) [2] H. Yu et al., IEDM (2016) [3] B. Yang et al., ISTDM (2012) [4] H. Miyoshi et al., VLSI (2014) [5] Kim et al., APE, 4, (2011) [6] A. Nayfeh et al., APL, 85 (2014) [7] H. Yu et al., EDL, 36 (2015) [8] J. Lin et al., TED, 63 (2016) [9] J. E. Ayers et al., JCG, 135 (1994) [10] R. M. Iutzi, E. A. Fitzgerald, APL, 107 (2015) [11] S. Pal et al., JAC, 645 (2015)

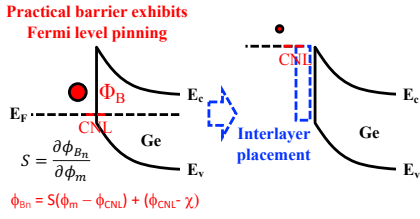


Fig. 1. Barrier height for n-Ge is $\sim 0.6\text{eV}$ ($S \sim 0.05$) due to Fermi level pinning^[1]. We propose III-V as an interlayer by redirecting CNL and exploiting low effective mass for high electron transmission.

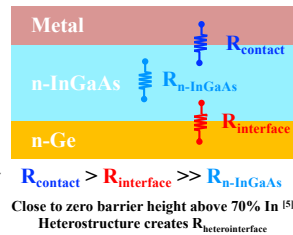


Fig. 2. Schematic of the heterocontact. $R_{\text{heterointerface}}$ plays an important role in overall ρ_c at

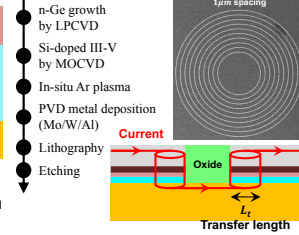


Fig. 3. Process flow of MRCTLM structure^[2]. Ge was doped either by in-situ PH_3 ($5 \times 10^{18}\text{cm}^{-3}$) or P I. I. ($3 \times 10^{19}\text{cm}^{-3}$).

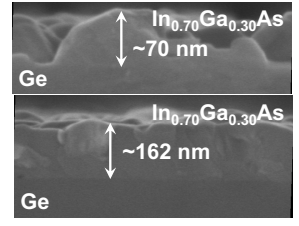


Fig. 4. SEM of III-V/Ge. 3D island growth was observed due to large lattice mismatch.

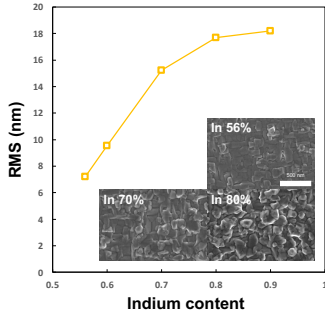


Fig. 5. Surface roughness of III-V/Ge. RMS monotonically increases with In %. In-plane SEM of III-V grown on Ge.

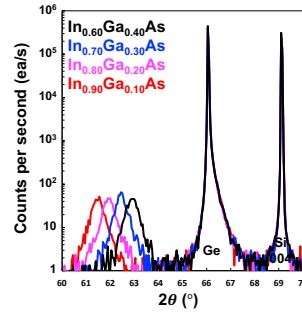


Fig. 6. III-V and Ge were integrated on Si, confirmed by XRD $2\theta - \omega$ scan. Large FWHM of III-V is indicative of defective layers.

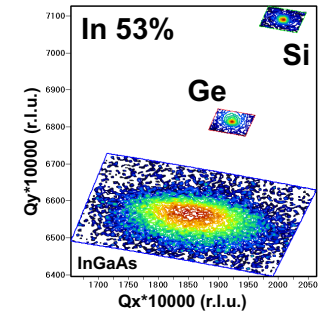


Fig. 7. XRD Reciprocal space mapping. III-V was confirmed to have 0% strain. Large mosaicity due to complete strain relaxation.

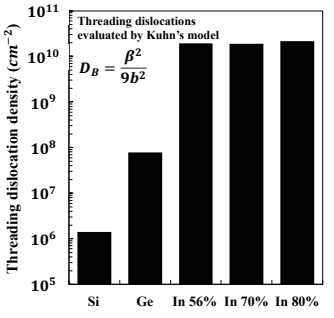


Fig. 8. Estimated dislocation densities of Si, Ge, and III-V from ω scan. Random distribution and 60° TD in (111) plane were assumed.

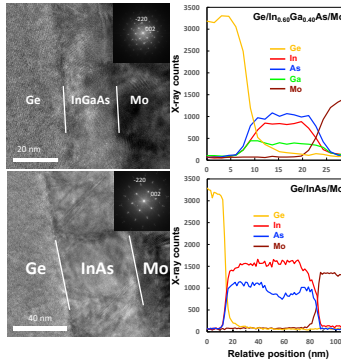


Fig. 9. HRTEM & EDS of 60% In and InAs. Strain relaxation and defects were captured in diffraction pattern. Diffusion of Ge into III-V was observed.

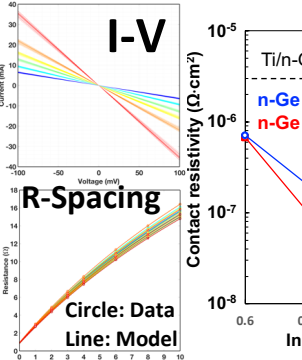


Fig. 10. ohmic behavior of the heterocontact. ρ_c was extracted from resistance vs. spacing.

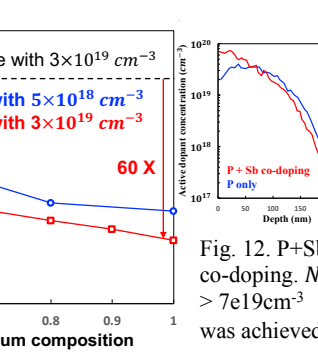


Fig. 11. ρ_c vs. In composition with different N_d . The blue line and the red one correspond to Ge with $5 \times 10^{18}\text{cm}^{-3}$ (in-situ PH_3) and $3 \times 10^{19}\text{cm}^{-3}$ (I. I.), respectively. 60X improvement was achieved in the heterocontact at N_d of $3 \times 10^{19}\text{cm}^{-3}$.

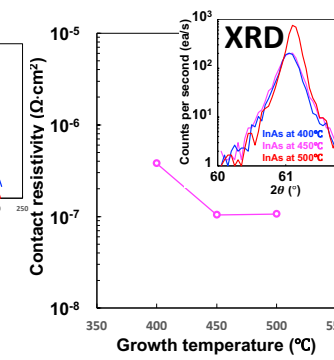


Fig. 13. InAs grown on Ge with $5 \times 10^{18}\text{cm}^{-3}$ at different temperatures. Low temperature growth results in smoother surface, but less N_d , thus, $\rho_c \uparrow$.

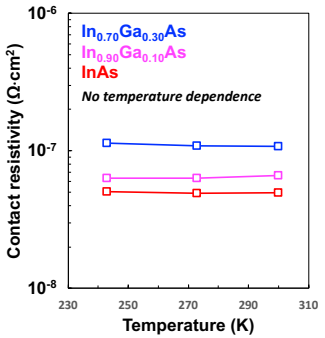


Fig. 14. Temperature dependence of the heterocontacts with various In % showing that ρ_c is almost invariant to temperature.

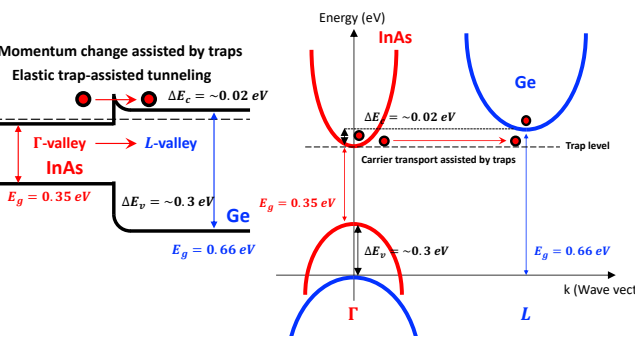


Fig. 15. Band and E-k diagrams of the heterocontact. Conduction band offset (InAs/Ge) is $\sim 0.02\text{eV}$ ^[11]. Carriers may transit to the other valley at the heterointerface by elastic trap-assist tunneling through defect states, which is temperature independent. Momentum shift is assisted by traps from dislocations.

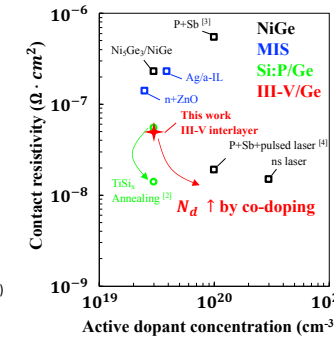


Fig. 16. Benchmark of ρ_c as a function of Ge N_d . Co-doping will be delayed^[3].